Artificial Intelligence

2

Improving TLD Personnel Dosimetry of Occupational Workers

Munir S. Pathan, S. M. Pradhan and T. Palani Selvam*

Radiological Physics and Advisory Division; Health, Safety & Environment Group, Bhabha Atomic Research Centre, Trombay – 400085, INDIA

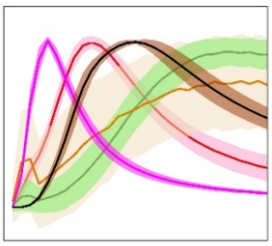

Different Classes of Glow Curves of $CaSO_4$:Dy

ABSTRACT

Thermoluminescence dosimeter (TLD) based personnel monitoring is widely employed for recording occupational radiation doses. TLDs used in routine monitoring are subjected to diverse field conditions, including processing and handling that result in variability in the glow curve (GC) shape. The distortions in the shape of GC may lead to variations in the estimated dose. The present work is focused on: (a) investigation and classification of anomalies in GC using machine learning algorithms, (b) development of an artificial intelligence (AI) based decision support system for screening GCs, and (c) providing a predictive maintenance system for the TLD badge reader.

KEYWORDS: *Personnel monitoring, Glow curves, Machine learning*

Introduction

Luminescence-based dosimeters have been used in radiation dosimetry for decades. The property of emission of luminescence signal proportional to received radiation exposure makes the luminescence dosimeters suitable for radiation personnel monitoring as well as other radiation dosimetry-related applications. Hence, Thermoluminescence (TL)-based dosimeters are one of the most commonly used dosimeters in personnel monitoring of occupational workers. In India, about 0.25 million occupation workers are monitored for external exposure to ionizing radiation (beta, gamma and x-rays) using $CaSO_4$:Dy-based TLD badges [1-3]. Presently, 16 TLD personnel monitoring laboratories provide TLD services across our country. The TLD badges are read using semiautomatic TLD badge readers that utilize hot N_2-gas-based clamped heating for stimulation of TL dosimeters [4].

The Glow Curves (GCs) recorded in routine measurements may not always show the ideal characteristic shape. Various types of anomalies may appear from various sources like dosimeter, reader, zero dose signal, etc. At lower doses, the non-radiation-induced TL signal, originating due to the black body radiation from heated reader components and the dark current from the photomultiplier tube (PMT), causes the deviation in the shape of GC [5, 6].

The TLD reader-related factors such as variation in heating rate, cross-talk due to sequential heating [7], etc. may lead to deformities in the shape of GC. Other factors like dirt/dust/oil on the TL element, the coloration of the TL element, corrosion of the TLD card, aberration due to scratch/stress on the TL element, etc. also cause deformities in the shape of GC [8]. Hence, in routine personnel monitoring, screening of GCs is a mandatory procedure before dose computation.

Recent studies on the application of Machine Learning (ML) for anomalous GC identification, and estimation of elapsed time after exposure for LiF:Mg:Ti-based TL dosimeters have shown an impressive improvement in dosimetric outcomes [9-11]. In this work, we demonstrated the applicability of different ML algorithms for the identification of abnormal GCs as well as the classification of GCs based on associated abnormalities for the $CaSO_4$:Dy-based personnel monitoring system. Further, an R-shiny based web-application is developed to deploy the ML models for routine TLD personnel monitoring. With implementation of ML algorithm about 99% classification accuracy with minimization of subjectivity and increase in the throughput of personnel monitoring laboratory can be achieved.

Materials and Methods

TLD personnel monitoring system

The TLD Badge comprises a TLD card and Cassette. The TLD card consists of three $CaSO_4$:Dy-Teflon discs of thickness 0.8 mm and diameter 13.3 mm, and are mechanically clipped to a Nickel-plated Aluminium plate. The TLD cards are loaded in the cassette with filters to compensate for the energy dependence and to provide a gross estimation of energy/type of radiation [12]. To estimate the dose, the TLD badges are read using a semiautomatic TLD badge reader. Thermal stimulation is delivered using hot N_2 gas-based clamped heating to obtain the TL signal from the pre-irradiated dosimeter.

Dataset preparation

A dataset of ~3000 experimental GCs comprising the normal GCs, residual TL GCs, annealed background GCs, GCs with spikes, and delayed/early peak GC is prepared. The number of anomalous GC in the experimental dataset is limited due to the seldom occurrence of anomalies in routine monitoring, ~1500 GCs with anomalies are generated by simulation. For the simulation of GCs, the time-temperature profile of the TL element is simulated. The hot N_2 gas incident on the TL-element delivers heat to the TL element via forced convection. During the heating cycle, the TL element loses some heat to the surroundings due to the finite temperature

*Author for Correspondence: T. Palani Selvam
E-mail: pselvam@barc.gov.in

difference. The heat exchanges between hot gas, TL element, and surrounding is given in the following rate equation [13].

$$\frac{dT_d}{dt} = \frac{1}{C_d}\left(\frac{dH_d}{dt} - \frac{dH_s}{dt}\right) \quad (1)$$

Where dH_d/dt is the rate of heat transferred from hot gas to disc (Js^{-1}), dHs/dt is the rate of heat transferred from heated disc to surrounding (Js^{-1}) and C_d is heat capacity of the disc ($J^\circ K^{-1}$).

$$\frac{dH_d}{dt} = P_d\,(T_g(t) - T_d(t)) \quad (2)$$

$$\frac{dH_s}{dt} = P_s\,(T_d(t) - T_{sr}) \quad (3)$$

Where $T_g(t)$ is the temperature of the gas, $T_d(t)$ is the temperature of the disc at time t ($^\circ K$), T_{sr} is temperature of surrounding ($^\circ K$), P_d is the thermal conductance of heated gas and disc interface ($J^\circ K^{-1}s^{-1}$), Ps is thermal conductance of disc and surrounding interface ($J^\circ K^{-1}s^{-1}$). Using the above equations (1 – 3), the time-temperature profile of the disc can be given by the following equation

$$\frac{dT_{disc}(t)}{dt} = \alpha(T_g(t) - T_d(t)) - \alpha'(T_d(t) - T_{sr}) \quad (4)$$

Where, $\alpha = P_d/C_d\,(s^{-1})$, $\alpha' = P_s/C_d\,(s^{-1})$, α' represents heat loss to surrounding.

Further, equation (4) is modified to account for radiative heat loss and gain via black body radiation from TL element to surrounding and surrounding to TL element respectively [14].

$$\frac{dT_{disc}(t)}{dt} = \alpha(T_g(t) - T_d(t)) - \alpha'(T_d(t) - T_{sr}) - \lambda_1 T_d(t)^4 + \lambda_2 T_{sr}^4 \quad (5)$$

Where Tsr is the temperature of the surrounding ($^\circ K$), λ_1 and λ_2 are constants having dimensions ($^\circ K^{-3}s^{-1}$). The rate equation given by equation (5) is solved numerically by the finite difference method to obtain the temperature profile of the TL element. The glow curve of $CaSO_4$:Dy was simulated using the Randall-Wilkins model as given in equation (6) [15].

$$I(t) = -\frac{dn}{dt} = cn^b fe^{\left(-\frac{E}{kT_{d(t)}}\right)} \quad (6)$$

Where I(t) is TL intensity at time t, n is number density of trapped carriers (m^{-3}), b is order of kinetics, c is reader response factor (counts/TL intensity), E is activation energy (eV), f is frequency factor/pre-exponential factor (s^{-1}), k is Boltzmann constant ($J^\circ K^{-1}$).The ten-trap model is used for the simulation of the composite GC for clamped/exponential heating [16]. The simulated composite GC (blue line) and contributing peaks (dashed lines) along with experimental GC (pink line + markers) are shown in Fig.1.

The anomalous GC of early/delayed peak are simulated by altering the temperature profile by varying the value of the parameter "α". Fig.2 shows the different types of GCs and variability in their shapes.

ML model tuning and evaluation

Supervised machine learning is the process of training a function/s to map an input to the output using the known output for a supplied set of inputs. It improves itself iteratively by comparing the estimated output to the desired ones and accordingly adjusting the parameters. In present work, we investigated three competing supervised learners for the classification of abnormal GCs, Viz. Artificial Neural Network (ANN), Support Vector Machine (SVM), and Random Forest (RF). The Hyperparameters of ANN such as activation function, number of nodes/layers, learning rate, optimization method, etc. are tuned to obtain optimum classification accuracy. To obtain the accurate RF model, number of parameters (features) to be sampled randomly for each decision tree and the number of trees to be grown under a forest is tuned. Similarly, the SVM algorithm is optimized by tuning parameters like a penalty, margin, kernel, etc. The accuracy of classification of GCs is compared for all optimized ML models for selection of best of three algorithms.

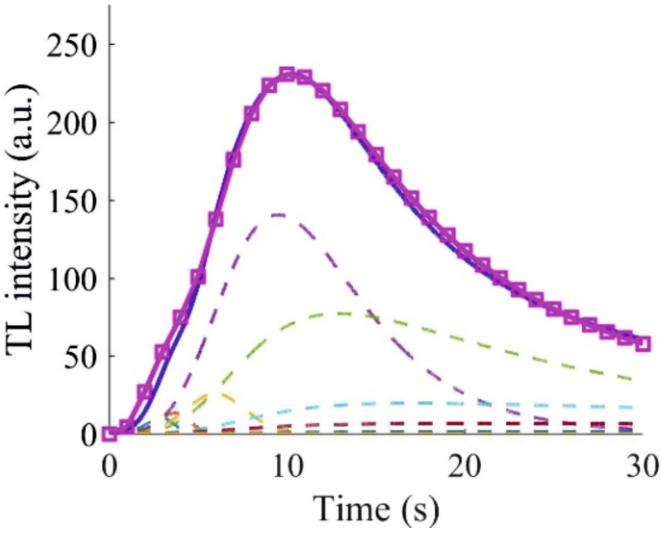

Fig.1: Simulated and experimental GC.

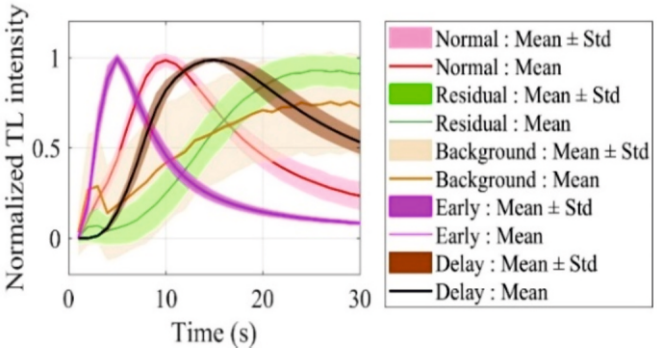

Fig.2: GCs of different class from dataset.

Deployment of ML model

The selected ML model is deployed into routine personnel monitoring by integrating it with a graphical user interface (GUI) using R-shiny. The TLD badge reader software provides the GC files in *.txt or *.xlsx file format, these files consist of the cumulative TL counts at every second, N_2-gas temperature, personnel number, TLD card ID, disc position and card position. These GC files are imported into the supplied as input after pre-processing to ML model. The models returns a data frame of class and probabilities of GCs. To diagnose the health of the TLD badge reader, the average probability of all normal GCs and a pie chart of the proportions of each class are generated. In addition to the GC screening, the software provides the dose calculation tool that searches and averages the control/background TL counts for a period of use of a particular institution, calculates net TL counts, and estimates dose as well as the type of radiation to which the TLD badge is exposed.

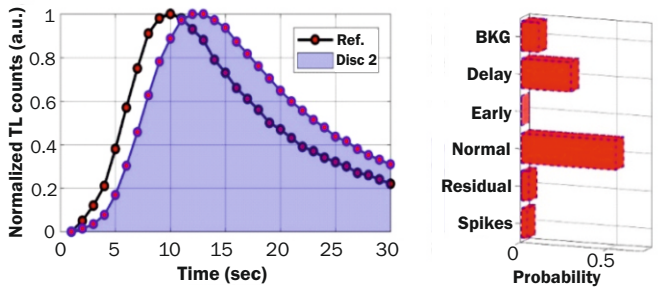

Fig.3: Delayed peak GC and its class probabilities.

Table 1: Comparison of the accuracy of algorithms.

Models	ANN	SVM	RF
Accuracy	0.9666	0.9611	0.9905

Results and Discussion

Identification of anomalous GC

The GCs are classified into six classes as per the type of GC and associated anomaly, viz. Normal GC, Annealed background, Residual GCs, Early peak GC, Delayed peak GC, and spikes in GC. The performance of each algorithm is analysed using a set of parameters as shown in Table 1.

The overall accuracy achievable for the test dataset from the RF algorithm is higher than that of ANN and SVM. Therefore, RF model is used for the development of application for screening of GCs. The RF model provides the probability of each class for a particular GC, the probability of a normal class between 0.8 and 1 is considered to be acceptable. If the probability of the normal class is less than 0.7, then significant deviation from the standard GC shape are observed. Fig.3 shows an example of normal GC with a slightly delayed peak indicating insufficient heating of the TL element, even though the GC is classified as normal GC, the probability of normal class is less than 0.75 and the probability of delayed peak is significant.

Further to validate the effectiveness of the use of probability as an indicator of TLD reader health, an experiment was conducted by decreasing the flow rate of N_2-gas by 20 %, and TLD cards exposed to various doses are read on such TLD readers. The average class probabilities of GCs of each disc from a normal TLD reader and faulty (simulated) TL are depicted in Fig.4. For normal TLD badge reader, the average probability of the normal class of GC is between 0.8 – 1 and for the rest of the classes it is negligible for all three discs. Similarly, for faulty TLD reader, the average probability of a normal class of GC is less than 0.7, indicating a major deviation in the shape of GCs. The average probability of delayed peak is significant, which indicates probable under-heating of TL elements.

AI-based GC screening tool

The screenshot of GUI is shown in Fig.5, the sidebar panel provides browsing, reader software selection, TL count threshold, probability threshold and combined ML + analytical decision [8] making options. The main window consists of several tabs, Viz. graphical, tables, analysis, summary, dose from GC and dose from dump. The graphical tab shows information related to TLD card like personnel number, card ID and readout date and three figures showing the plot of GC along with the class of GC, total TL counts and probability of normal class.

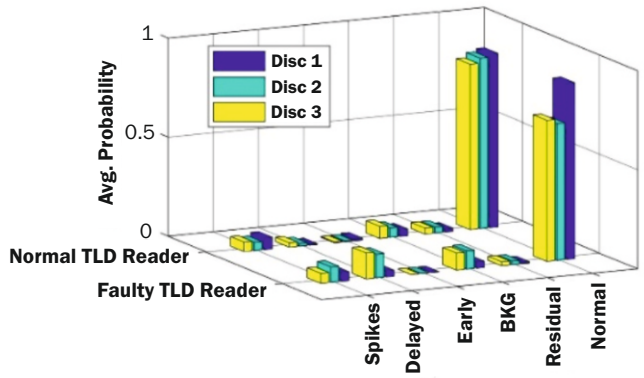

Fig.4: Mean class probability of normal GCs.

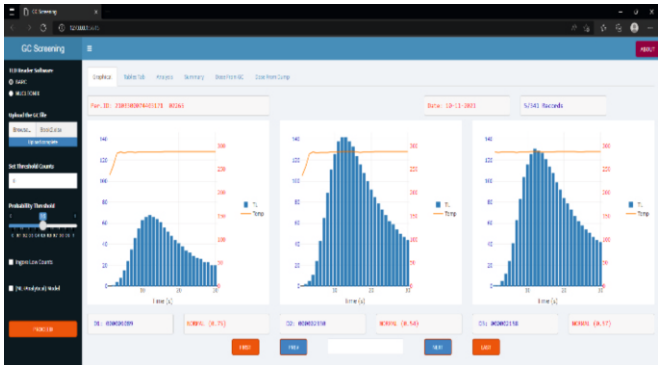

Fig.5: Screenshot of the graphical tab of GC screening software.

Conclusion

In routine personnel monitoring, thousands of cards are processed monthly and it needs to be ensured that the dosimetric accuracy is not compromised. The dosimetric accuracy mostly relies on the accuracy of the signal i.e. GC. With the continuous increase in the number of monitored occupational workers, there is a need for automation to increase the throughput of TLD personnel monitoring laboratories without compromising dosimetric accuracy. Therefore, the application of ML algorithms into the GC-screening process which is one of the mandatory steps in TLD processing will surely improve the throughput of the laboratory. Also, with human intervention, the variability in decisions about the correctness of GC results in subjectivity. The subjectivity can also be minimized with the use of AI-based algorithms. Further, the use of a probabilistic approach gives an insight into the anomaly as well as provides a health diagnosis of the TLD reader which serves as predictive maintenance system.

References

[1] K .G. Vohra, et al., A personnel dosimeter TLD badge based on $CaSO_4$: Dy Teflon TLD discs. Health Physics, 1980, 38(2), 193-197.

[2] A. S. Pradhan, and R. C. Bhatt, Metal filters for the compensation of photon energy dependence of the response of $CaSO_4$:Dy - Teflon TLD discs. Nuclear Instruments and Methods, 1979, 166(3), 497-501.

[3] A. S. Pradhan, B. C. Bhatt and K. Ayyangar, Development of $CaSO_4$: Dyteflon discs thermoluminescence dosimetry. in Proceedings of the national symposium on thermoluminescence and its applications, Kalpakkam, February 12-15, 1975, 1976.

[4] M. S. Kulkarni, P. Ratna and S. Kannan, A new PC based semi-automatic TLD badge reader system for personnel monitoring. in Proceedings of International Radiation Protection Association Conference, Hiroshima, Japan, 2000.

[5] Van Dijk, J. W. E., Uncertainties in personal dosimetry for external radiation: a Monte Carlo approach. Radiation Protection Dosimetry, 2006, 121(1), 31-38.

[6] Van Dijk, J. W. E. and Al Busscher, F, The zero signal and glow curves of bare LiF: Mg, Ti detectors in a hot gas TLD system. Radiation Protection Dosimetry, 2002, 101(1-4), 59-64.

[7] M. S. Pathan, et al., Study of effect of consecutive heating on thermoluminescence glow curves of multi-element TL dosemeter in hot gas-based reader system. Radiation Protection Dosimetry, 2019, 187(4), 509-517.

[8] S. M. Pradhan, C. Sneha, and M. M. Adtani, A method of identification of abnormal glow curves in individual monitoring using $CaSO_4$: Dy Teflon TLD and hot gas reader. Radiation Protection Dosimetry, 2011, 144(1-4),195-198.

[9] A. Gal and H. Datz, Automatic detection of anomalous thermoluminescent dosimeter glow curves using machine learning. Radiation Measurements, 2018, 117, 80-85.

[10] A. Gal and H. Datz, Improvement of dose estimation process using artificial neural networks. Radiation Protection Dosimetry, 2019, 184(1), 36-43.

[11] Kröninger, Kevin, et al., A machine learning approach to glow curve analysis. Radiation Measurements, 2019, 125, 34-39.

[12] D. Datta, et al., HANDBOOK ON TLD-BASED PERSONNEL MONITORING (REV. 1-2018), in BARC Report. 2018, Bhabha Atomic Research Centre: BARC Press, Mumbai.

[13] T. M. Piters and A. J. J. Bos, Effects of non-ideal heat transfer on the glow curve in thermoluminescence experiments. Journal of Physics D: Applied Physics, 1994, 27(8), 1747.

[14] H. Stadtmann, A. Delgado and J. M. Gómez-Ros, Study of real heating profiles in routine TLD readout: Influences of temperature lags and non-linearities in the heating profiles on the glow curve shape. Radiation Protection Dosimetry, 2002, 101(1-4), 141-144.

[15] G. Kitis, J. M. Gomez-Ros and Tuyn, W. N. Jan Thermoluminescence glow-curve deconvolution functions for first, second and general orders of kinetics. Journal of Physics D: Applied Physics, 1998, 31(19), 2636.

[16] J. H. Souza, L. A. R. Da Rosa and C. L. P. Mauricio, On the thermoluminescence glow curve of $CaSO_4$: Dy. Radiation Protection Dosimetry, 1993, 47(1-4), 103-106.